TECHNISCHE MECHANIK, 32, 2-5, (2012), 205-220
submitted: October 30, 2011

A Microstructure Sensitive Approach for the Prediction of the Creep Behaviour and Life under Complex Loading Paths

J. Ghighi, J. Cormier, E. Ostoja-Kuczynski, J. Mendez, G. Cailletaud, F. Azzouz

The prediction of the creep behaviour and life of components of aeronautic engines like high pressure turbine blades is still a challenging issue due to non-isothermal loadings. Indeed, certification procedures of turboshaft engines for helicopters consist of complex thermomechanical histories, sometimes including short and very high temperature excursions close to the γ'-solvus (T~1200°C) of the blade alloy. A better design of those components could be gained using a model that takes into account non-isothermal loadings inducing microstructural changes.
Most of the commonly used models consider only a nearly constant (or slowly evolving) microstructure, i.e. far from the rapid microstructure evolutions encountered during close γ'-solvus overheatings where a rapid dissolution/precipitation of the γ'-phase and fast recovery mechanisms were observed by Cormier et al. (2007b). A new constitutive modelling approach was hence recently proposed in a crystal viscoplasticity framework to capture the transient effects of such rapid microstructure evolutions on the creep behaviour and life (Cormier and Cailletaud (2010a)).
In this article, an updated version of this model is detailed. Special attention will be paid to (i) the effect of the accumulated plastic strain on the microstructure evolution, (ii) the introduction of an additional damage formulation, and (iii) the creep strain at failure. The performances of the model are illustrated on the basis of isothermal or complex non-isothermal creep experiments performed on nearly [001] oriented samples.

1. Introduction

Nickel-base single crystal superalloys are widely used for of aero-engines or industrial gas turbine components such as high pressure turbine blades and vanes due to their excellent high temperature properties (see e.g. Reed (2006)). These very good mechanical properties are inherited from the absence of any deleterious grain boundaries and from their unique microstructure which consist of a high volume fraction (approximately 70%) of cuboidal γ'-precipitates coherently merged in a γ matrix, the γ' precipitates being very efficient barriers to the motion of dislocations at high temperature thermomechanical loadings.
The prediction of the creep behaviour and life of components of aeronautic engines like high pressure turbine blades is still a challenging issue due to non-isothermal loadings. A variety of constitutive models, using either microstructure or phenomenological considerations, have been developed for the simulation of the creep behaviour of Ni-based single crystal superalloys at high temperatures, see e.g. Norton (1929), Svoboda and Lukás (1998), McLean and Dyson (2000), Leidermark et al. (2009).
The most recent models use a crystal plasticity framework in order to take into account the effect of crystallographic anisotropy on the creep properties (Han et al. (2010)). Moreover, the addition of new internal variables which represent, for example, particles dissolution/precipitation or dislocation recovery mechanisms, allows for a better prediction of the high temperature inelastic behaviour when the microstructure is likely to evolve. For example, taking in account high temperature microstructure evolution such as the γ' directional coarsening (the so-called γ'-rafting) allows a quite good modelling of the high temperature/low stress creep behaviour (MacLachlan et al. (2001)) or the induced softening under cyclic loading (Fedelich et al. (2009)). On the other hand, the consideration of the evolution of mobile and pinned dislocations densities allows for a good prediction of both viscoplastic and rate-independent plastic behaviour, as recently proposed by Staroselsky and Cassenti (2011) (see also Staroselsky and Cassenti (2008), (2010)). Finally, considering both kinds of approach, i.e. the evolutions of the mobile and sessile dislocations densities on one hand, and the consideration of the γ'-rafting kinetics on the other hand, allows for a description of the creep behaviour over a wide range of temperatures involving very different deformation mechanisms and subsequent creep curve shapes, as suggested Fedelich (2002) in his constitutive model.
However, none of the above-mentioned approaches is designed to reproduce complex temperature histories involving transient mechanical states. Indeed, the weakness of these models is that the material is always considered to be at equilibrium. Thus, the kinetics of microstructure evolutions encountered during/after close γ'-solvus overheatings where dissolution/precipitation of the γ'-phase and fast recovery mechanisms phenomena occur are not taken into account, see e.g. Cormier et al. (2007b).

The aim of the present article is to propose an improved version of a crystal plasticity model in which creep behaviour and damage evolution are coupled. Compared to classical viscoplastic models, our approach is enriched with new internal variables which explicitly account for microstructure evolutions. The present article describes viscoplastic constitutive equations which are able to take into account the non-isothermal creep behaviour under γ'-dissolution/precipitation conditions and it presents an extension of the Polystar model recently developed by Cormier and Cailletaud (2010a).

The paper is organized as follows: Section 2 shows the original constitutive equations of the model Polystar. Section 3 focuses on the newly introduced internal variables which improved the original Polystar model. Finally, Section 4 illustrates how the updated Polystar model performs during a complex mission, and the remaining limitations of the model in its present form.

2. Original Formulation of the Polystar Model

2.1. Nomenclature

Latin

a^* : temperature dependant recovery variable
B : Burgers vector magnitude
d_c^s : damage scalar on slip system s
d_{dislo} : damage associated with an increase of the mobile dislocations density
e_{cfl} : creep strain accounting for the dislocation density saturation in the matrix
f_{equ} : volume fraction of the γ' phase at thermodynamical equilibrium
f_l : large γ' precipitates volume fraction
f_s : small γ' precipitates volume fraction
G : shear modulus (= C_{44})
h_{sj} : components of the interaction matrix
$\underline{l}^s$: slip direction in the slip plane
$\underline{\underline{m}}^s$: orientation tensor
$\underline{n}^s$: normal to the slip system plane
Q : blocked dislocation hardening
Q* : dislocation hardening which can be recovered during an overheating
r^s : isotropic hardening on slip system s
$\dot{T}$: heating/cooling rate
w_{001} : γ channel width along the [001] direction

Greek

α^s : kinematic state variable on slip system s
$\underline{\underline{\varepsilon}}^p$: viscoplastic strain tensor
γ^s : viscoplastic shear on slip system s
ρ^s : isotropic state variable on slip system s
υ : isotropic state variable on slip system s
$\underline{\underline{\sigma}}$: applied stress tensor
τ^s : resolved shear stress on slip system s
ω^s : kinematic-type hardening associated with the damage d_c^s on slip system s

2.2. Equations

The model is a phenomenological microscopic-macroscopic model based on the pioneering rate-dependent single crystal plasticity theory of Peirce et al. (1982) and developed by Cailletaud (1992) with isotropic and kinematic hardenings. Indeed, Polystar model is formulated in a crystal plasticity framework. The plastic strain rate tensor $\dot{\underline{\underline{\varepsilon}}}^{p}$ is, as usually in such a framework, dependent on the slip rate of each slip system $\dot{\gamma}^{s}$, the orientation tensor $\underline{\underline{\underline{\underline{m}}}}^{s}$ and the sign of shear on each system τ^{s} (Eq. (1)).

$$\dot{\underline{\underline{\underline{\underline{\varepsilon}}}}}^{p} = \sum_{s} \dot{\gamma}^{s} \underline{\underline{\underline{\underline{m}}}}^{s} sign\left(\tau^{s}\right) \tag{1}$$

The shear on each slip system depends on the stress tensor $\underline{\underline{\sigma}}$ and the orientation tensor in the following way

$$\tau^{s} = \underline{\underline{\sigma}} : \underline{\underline{\underline{\underline{m}}}}^{s} \tag{2}$$

The orientation tensor is defined as follow, $\underline{n}^{s}$ and $\underline{l}^{s}$ being the normal to the slip plane and the slip direction in the slip plane, respectively

$$\underline{\underline{\underline{\underline{m}}}}^{s} = \frac{1}{2}\left(\underline{n}^{s} \otimes \underline{l}^{s} + \underline{l}^{s} \otimes \underline{n}^{s}\right) \tag{3}$$

Modelling the creep behaviour of Ni-based single crystal superalloys allow us to only consider the octahedral slip systems, since cube slip, especially at temperatures greater than 900°C, is not a relevant deformation mechanism, even for <111> oriented superalloy single crystals, as already observed by Sass et al. (1996) and Han et al. (2010) under isothermal creep conditions. Moreover, recent results obtained on <111> oriented MC2 samples under non-isothermal creep-fatigue loading by Le Graverend et al. (2010) clearly suggest that the main active slip systems at 1050°C are octahedral ones.

A Norton flow rule gives the shear strain on each slip system $\dot{\gamma}^{s}$, including a damage coupling by means of d_c^{s}

$$\dot{\gamma}^{s} = \left(\frac{f^{s}}{K\left(1 - d_c^{s}\right)}\right)^{n} \tag{4}$$

By using such a coupling, the impact of damage on the increase of the plastic strain rate is, by nature, anisotropic. The yield criterion f^{s} is usually defined as the difference between the shear stress τ^{s} and the hardenings (isotropic r^{s} and kinematic x^{s}). But this latter hardening is useless in case of pure creep modelling, see e.g. Vladimirov et al. (2009). The yield function is hence defined by means of Eq. (5)

$$f^{s}\left(\tau^{s}, r^{s}\right) = \left|\tau^{s}\right| - r^{s} \tag{5}$$

Finally, the accumulated plastic strain rate $\dot{\upsilon}$ has a usual formulation

$$\dot{\upsilon} = \left(\left(\frac{2}{3}\right)\dot{\underline{\underline{\varepsilon}}}^{p} : \dot{\underline{\underline{\varepsilon}}}^{p}\right)^{1/2} \tag{6}$$

The Polystar model was developed in order to be able to reproduce the creep behaviour encountered under complex thermomechanical loadings representative of some ratings of high-pressure turbine blades where fast γ'-phase transformations are likely to occur during an overheating, for example. The impact of such temperature peaks on the mechanical behaviour has been studied in more details in Cormier et al. (2007b), (2008).

Thus, the microstructure evolutions that undergoes the material are introduced in the isotropic hardening r^{s}.

The evolution of the back stress has been decomposed into three terms (see Eq. (7)). Two non conventional variables related to crystal plasticity are introduced in this equation: Q^* accounts for the dislocation back-stress evolution during temperature changes, and w_{001} represents the γ channel width along a [001] crystallographic direction in a (100) or (010) plane.

$$r^s = r^0 + b\left(Q + Q^*\right)\sum_j h_{sj} \times \rho^j + \sqrt{\frac{2}{3}}\frac{\mathrm{GB}}{w_{001}} \tag{7}$$

The first term r^0 accounts for the initial size of the elastic domain and, from a metallurgical point of view, basically corresponds to the γ-matrix solid solution hardening. The second one is a work hardening parameter and the last one is a structural hardening term, also known as the Orowan stress the γ-matrix dislocations have to overcome to by-pass the γ' particles. ρ^s is a regular isotropic state variable which represent a critical dislocation density that can enter the γ-channels as proposed by Probst-Hein et al. (2001). This variable is described as a function of the accumulated plastic strain on each slip system

$$\dot{\rho}^s = \left(1 - b \times \rho^s\right) \times \dot{\gamma}^s \tag{8}$$

The dislocation density evolutions occurring during and after an overheating have been modelled according to Eqs. (9) and (10). Two main terms are considered in the work hardening: Q is a temperature-dependent material parameter which describes the dislocation pinned at the γ/γ' interface, while Q^* accounts for the dislocation density recovery occurring during overheatings. Q^* is a function of the maximum recoverable dislocation back-stress Q_{s0} and depends on the heating/cooling rates and on the overheating length by means of a^* (Eq. (10))

$$Q^* = a^* \times Q_{s0} \tag{9}$$

$$\dot{a}^* = -\frac{a^*}{\alpha^*}\dot{T} - \frac{a^*}{\beta^*} \tag{10}$$

The γ channel width evolution in the Orowan term is a function of the volume fractions of coarse and fine γ' particles (see e.g. Cormier et al. (2007a) and le Graverend et al. (2010)). This dependance has been determined experimentally using image analysis techniques. These analyses show that

- the γ channel width is depends on f_l , following a power law
- has been fixed to be linearly dependent on f_s

These observations are valid whatever the γ' microstructure (i.e. rafted or cuboidal) and whatever the thermomechanical history (i.e. isothermal or not). w_{001} is then expressed according to Eq. (11)

$$w_{001} = \frac{a_0}{\delta} \times \left[f_l^{m_1} - d_{tp} \times f_s\right] \tag{11}$$

In this equation, a_0 is the initial average edge length of the γ' cubes, and m_1, d_{tp} and δ are material parameters. The reader is referred to Cormier and Cailletaud (2010b) for additional details about this equation.

The evolution of the volume fraction of large γ'-precipitates f_l during heating or cooling periods in a temperature range inducing γ' dissolution is described by Eq. (12). An exponential expression is then given for the evolution of this kind of γ'-particles, as observed in MC2 alloy (Cormier et al. (2007a)). In this equation, f_{equ} is the γ' volume fraction at thermodynamical equilibrium which can be computed using Thermocal® calculations (Reed et al. (2007) for example) and α_l is a characteristic time for the γ' dissolution/precipitation. Both f_{equ} and α_l are temperature dependent.

$$\dot{f}_l = \frac{\left(f_{equ} - f_l\right)}{\alpha_l} \tag{12}$$

Considering the small precipitates, they are always observed after cooling from an overheating that has been performed in a temperature range inducing dissolution of the γ'-phase, whatever the orientation of the crystal. This is illustrated in Figure 1 for a non-isothermal creep test including a short overheating on the as-received microstructure for a [011] oriented MC2 sample. It is clearly observed that after a 30s overheating at 1200°C under 145 MPa followed by a fast cooling over 50°C/s, a hyperfine γ' precipitation whose average diameter is less than 15-20 nm is observed in the matrix in some large γ' precipitates free zones.

Moreover, since the small γ' precipitates do not have the same chemical composition as compared to the largest ones, their evolutions as a function of the temperature history cannot be simply written as the difference between f_{equ} and f_l. It was then decided to give different kinetics of dissolution, precipitation and coalescence for small precipitates (Cormier (2006)). Three cases are considered for the evolution of the volume fraction f_s of fine precipitates. First, considering isothermal conditions without overheating or during an overheating, the evolution is driven by a dissolution term in Eq. (13). Then, considering cooling after an overheating, the evolution of f_s is driven by a term of precipitation depending on the cooling rate $\dot{T}$ and one of dissolution in Eq. (14). Finally, considering re-heating after an overheating, the evolution is only driven by a dissolution term in Eq. (15).

$$\text{if } \left(f_{equ} - f_l\right) \le 0 \text{ then } \dot{f}_s = -\frac{f_s}{\alpha_s} \tag{13}$$

$$\text{if } \left(f_{equ} - f_l\right) > 0 \text{ and } \dot{T} < 0 \text{ then } \dot{f}_s = -\frac{f_{equ} - f_l - f_s}{\alpha_s}\dot{T} - \left(\frac{f_s}{K_{s1}}\right)^{m_s} \tag{14}$$

$$\text{if } \left(f_{equ} - f_l\right) > 0 \text{ and } \dot{T} \ge 0 \text{ then } \dot{f}_s = -\left(\frac{f_s}{K_{s2}}\right)^{m_s} \tag{15}$$

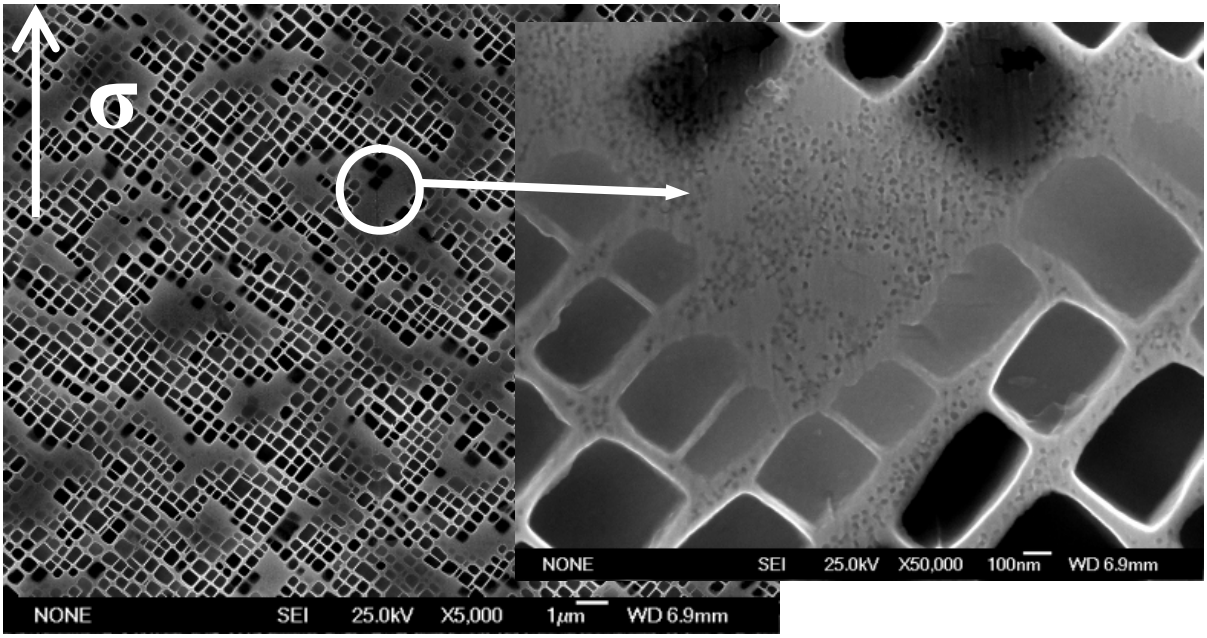

Figure 1: Hyperfine precipitates observed during a non-isothermal creep test after a short overheating (30s at 1200°C/145MPa), on the as-received microstructure of a [101] oriented MC2 sample. The arrow accounts for the loading direction.

As already pointed out in a previous part (see section 2.1), the Polystar model has a fully coupled formulation between the mechanical behaviour and the damage evolution. The damage rate is formulated at a microscopic scale (i.e. on each slip system) and is activated once a given creep strain threshold υ_d is reached in Eq. (16) (the motivation for such a threshold is analyzed in Cormier et al. (2008)). This damage law follows a Rabotnov-Kachanov type equation. However, instead of using a classical shear stress as the driving force for the damage

evolution, a new variable ω_s is used. ω_s has a formulation quite similar to a kinematic hardening (see Eq. (17) and Eq. (18)) as already suggested by Yu et al. (2008) and Wen et al. (2009). In fact, from the authors' point of view, the transition from the secondary creep stage (or "pseudo-secondary" creep stage under non-isothermal conditions) to the tertiary creep stage in the high temperature range (T > 1000-1050°C) for monocristalline Ni-based superalloys is mainly driven by a local increase of the density of mobile dislocations. In other words, the beginning of the tertiary creep stage at high temperature is due to microstructure evolution (e.g. γ' thickening, deformation pores nucleation and growth due to dislocation climb). In addition, any formulation considering the applied stress would not be able to account for the unconventional dependence of the MC2 alloy to a 1200°C overheating length where it was observed that the longer the overheating, the longer the post-overheating creep life (Cormier et al. (2008) and Cormier and Cailletaud (2010a)).

$$\text{if } \upsilon > \upsilon_d \text{ so } \dot{d}_c^s = \left(\frac{\left|\omega^s\right|}{K_x\left(1 - d_c^s\right)} \right)^{m_x} \tag{16}$$

$$\omega^s = C \times \alpha^s \tag{17}$$

$$\dot{\alpha}^s = \dot{\gamma}^s \times \left(sign\left(\tau^s - \omega^s\right) - d \times \alpha^s \right) \tag{18}$$

In those equations, K_x, C and d are three temperature-dependent parameters.

The Polystar model has been calibrated for the crystal orientation [001] by Cormier and Cailletaud (2010a) and both creep behaviour and lifetime are well predicted (see Figure 15 in Cormier and Cailletaud (2010a)) under isothermal and non-isothermal creep conditions. The identification of the model is based on an inverse identification procedure using standard optimization procedures. The material parameters introduced in Eqs. (11) to (15) are directly identified by metallurgical investigations. The reader is referred to Cormier and Cailletaud (2010a) for additional details about the identification of the model.

Nevertheless, some remaining limitations in this first version of this model were pointed out. Three of them have recently been solved and are detailed in the next section. Some additional efforts are under progress for two of them and will be exposed in the Section 4.

3. Improvements in the Non-Isothermal Creep Behaviour Modelling

Three of those limitations are corrected thanks to recent improvements of the model. They will be detailed in this section.

3.1. Effect of the Accumulated Plastic Strain on the γ' Dissolution/Precipitation Evolutions

A first limitation was already exposed in the paper of Cormier and Cailletaud (2010a) and concerns the effect of plastic strain on the γ'-evolutions such as dissolution kinetics. Indeed, the calculated accumulated plastic strain after an overheating performed on a virgin microstructure (i.e. without any creep deformation prior to an overheating) was proven to overestimate experimental creep strains monitored during the post-overheating creep stage. Such an overestimation is due to dissolution kinetics of the γ' phase which is only thermally driven through the temperature dependence of f_{equ} and α_l in Eq. (12) and which led to a wider γ channels and hence, easier plastic flow (through Eq. (7)). However, the γ' dissolution/precipitation kinetics is also plastic-strain dependent, and is slower for γ' cuboidal morphologies as compared to rafted ones. Such dependence was already proposed earlier in Cailletaud (1979) based on thermodynamics considerations. Since this γ' dissolution and precipitation are enhanced by the dislocation density at the γ/γ' interfaces due to pipe-diffusion (see e.g. Giraud et al. (2012) for γ' dissolution and Embury et al. (2003) for γ' precipitation), the updated Polystar model now includes a direct relationship between the evolution of coarse γ' volume fraction and the accumulated plastic strain υ. Equation (12) is now modified into Eq. (19).

$$\dot{f}_l = \left[1 - \delta_l \times \exp\left(-\frac{\upsilon}{e_{cfl}} \right) \right] \times \frac{\left(f_{equ} - f_l\right)}{\alpha_l} \tag{19}$$

e_{cfl} is a creep strain accounting for the dislocation density saturation in the matrix during creep and δ_l is a material parameter. In fact, during high temperature primary creep stage of Ni-based single crystals superalloys, the dislocation density progressively increases at the γ/γ' interfaces until a given dislocation density is reached (see, e.g., Probst-Hein et al. (2001)). This maximum number of dislocations allowed to penetrate γ channels corresponds to dislocations necessary to relax the misfit stresses, as well as those in excess of these "misfit dislocations" as proposed by Carroll et al. (2008). Once this maximum dislocation density is reached, creep deformation proceeds thanks to recovery mechanisms such as γ' shearing/annihilation at the opposite interfaces or dislocation climb at the γ/γ' interfaces (Sirinivasan et al. (2000) and Sarosi et al. (2007)). The result is that whatever the creep strains are reached, once this critical dislocation density at the γ/γ' interfaces is reached and the coherency stresses are relaxed, dissolution and precipitation kinetics hardly evolve.

An illustration of this improvement is shown in the Figure 2 where simulations, without and with the strain effect, after a 90 s overheating (denoted as OT in the figure) on the as-received microstructure (i.e. no creep prior to the overheating) are compared to its experimental counterpart. It is observed that a simulation with the updated version of the Polystar model exhibits a decrease of deformation as compared to the former version where the dissolution kinetics were calibrated to the deformed microstructures (i.e. rafted ones in this particular case). Here, since the accumulated plasticity induced by the initial OT is small enough, the dissolution kinetics is reduced, leading to a greater γ' volume content at the end of the overheating and to a subsequent lower amplitude primary creep stage, in good agreement with the experiment.

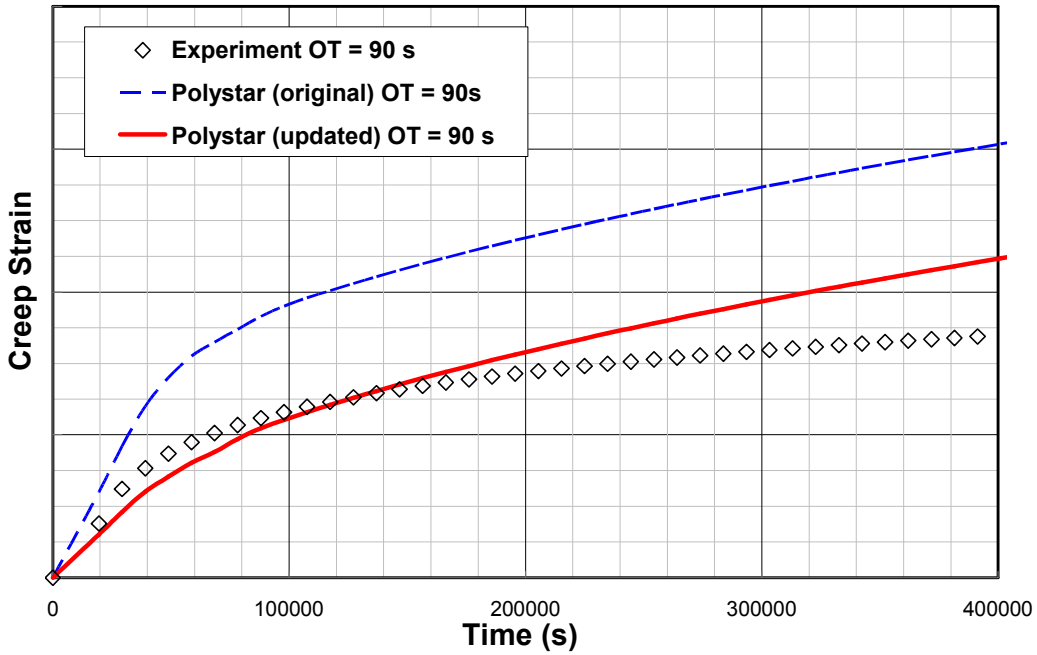

Figure 2: Model simulations of a non-isothermal creep test compared to an experimental result (symbols) for a 90s overheating occurring on the as-received microstructure (no creep before the temperature jump at 1200°C).

3.2. Low temperature (T < 1000°C) tertiary creep stage modelling

Another limitation encountered was the description of the tertiary creep stage encountered during "low" temperatures tests (<1000°C). Under such conditions, the tertiary stage is longer and more progressive as compared to the very steep tertiary creep stages encountered at high and very high temperatures (>1000°C) and corresponding to a highly localized failure. In order to improve the tertiary creep stage description for these conditions, a new source of damage has been added. A multiplicative damage of the Norton flow rule has been added to account for such progressive strain rate increase, as already proposed by McLean and Dyson (2000) and by Wen et al. (2009). Equation (4) is now transformed into Equation (20)

$$\dot{\gamma}^s = \exp\left(d_{dislo}\right) \times \left(\frac{f^s}{K\left(1 - d_c^s\right)} \right)^n \quad \text{with} \quad \dot{d}_{dislo} = C_{dislo} \times \dot{\gamma}^s \tag{20}$$

In this equation C_{dislo} is a temperature-dependent material parameter.

Such a damage accounts for the multiplication of mobile dislocations with the accumulated viscoplastic strain. It occurs under conditions where the so-called γ/γ' topological inversion can be encountered (see pioneering work of Fredholm (1987) or Link et al. (2000)). An illustration of such a topological inversion is provided in Figure 3 for an MC2 alloy after creep failure at 850°C/400 MPa. We can observe that the γ matrix (bright phase in Figure 3) is now embedded in the γ' phase.

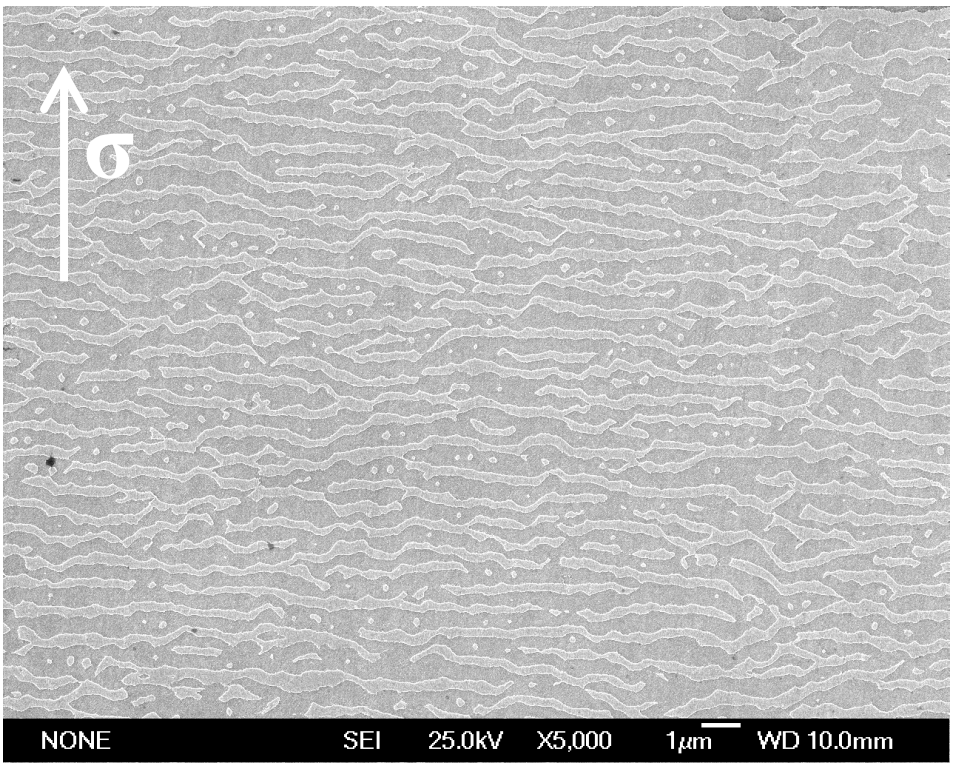

Figure 3: MC2 γ/γ' microstructure after creep failure at 850°C/400 MPa. γ' phase appears in dark. Note that the γ' phase is interconnected and surrounds the γ phase.

Two illustrations of the improvement obtained in the description of the tertiary creep stage are shown in Figure 4 where simulations (without and with multiplicative damage) of isothermal tests at 850°C and 950°C are compared to their experimental counterparts. It is observed that simulations with the enhanced Polystar model provide a better description of the progressive tertiary creep stages of these tests.

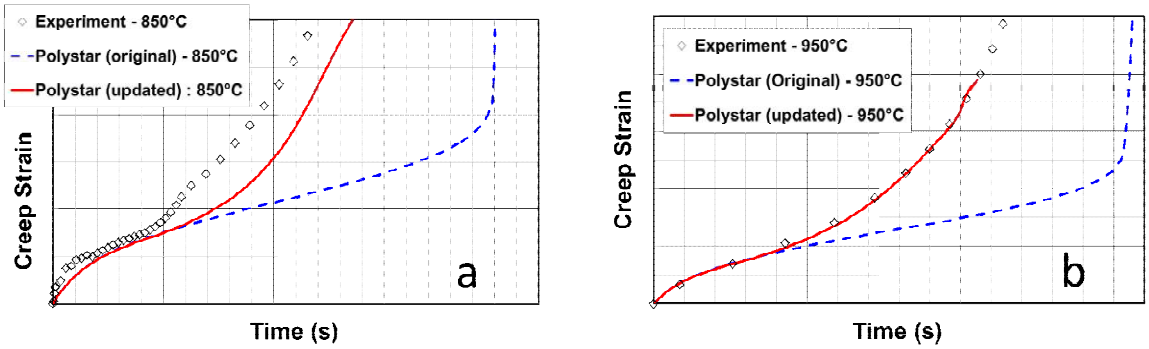

Figure 4: Models simulation of isothermal creep behaviour compared to experimental result (symbols) at 850°C (a) and 950°C (b).

3.3. Creep strain at failure

Finally, the last modification undertaken and presented in this article was performed in order to reach greater accumulated plastic strains at failure. Indeed, a difference was observed which can be as large as 10% in between experimental creep strains at failure and those obtained with the original Polystar model. In case of numerical simulations for conditions inducing a very steep tertiary creep stage corresponding to a highly localized failure process (i.e. high temperature/low stress conditions), correcting this difference would be useless. However, in case of the above mentioned progressive tertiary creep stages, having a better description of the tolerable creep strain at failure is very important during finite element simulations where large stress redistributions are likely to occur close to stress concentrators.
To achieve higher creep strains at failure, a kinematic-hardening type formulation of the damage evolution presented in Eq. (18) has been reconsidered. We added a dynamic recovery in Eq. (18) ($M(\alpha^s)^{m_\alpha}$ term) to induce a slower saturation of α^s, leading to Eq. (21).

$$\dot{\alpha}^s = \dot{\gamma}^s \times (sign(\tau^s - \omega^s) - d \cdot \alpha^s) - M(\alpha^s)^{m_\alpha} \tag{21}$$

An illustration of an improved result is shown in Figure 5 where simulations of an isothermal test without and with dynamic recovery are compared to their experimental counterpart. It is observed that simulation with the updated Polystar model exhibits an increase of the deformation at the failure highlighted by the vertical arrow in Figure 5.

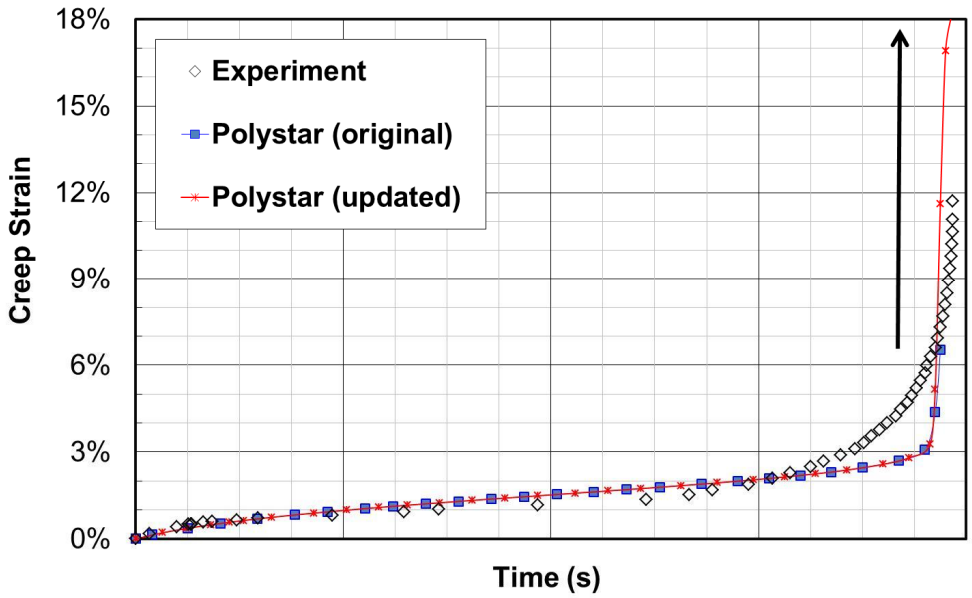

Figure 5: Model simulations of isothermal creep behaviour compared to experimental result (symbols).

The Polystar model with the above-mentioned improvements requires eight parameters for the mechanical evolutions, ten parameters for the damage evolution and ten parameters for the microstructure evolutions.

4. Complex Simulations and Future Improvements

In this section, the possible utilisations of the Polystar model for complex thermomechanical histories, as well as some residual limitations under the present enhanced formulation will be detailed. The two main present limitations of the model come from (i) the effect of γ' rafting on the mechanical properties and (ii) the crystal rotation which is occurring during plastic deformation for unstable orientations.

4.1. Simulation of Complex Missions

The Polystar model is currently used at Turbomeca to calculate creep strains and creep life of HP turbine blade airfoils under complex thermomechanical missions, such as ASMET ones. An illustration of such a mission is shown in Figure 6 where the first stage (Figure 6a) is cycled 100 times. Then, a stage including close γ'-solvus overheatings occurs (Figure 6b) prior to another 100 cycles as defined in Figure 6a.

The results of the simulation done with two different models are presented in Figure 7, using the Polystar model which takes into account history effects (i.e. dissolution/precipitation of γ' particles and dislocations recovery mechanisms) and another one which not consider these effects. In this last model, the thermomechanical loading is only taken into account through the dependence of the material parameters. Before the overheating sequence (Fig. (6b)), it is observed that the simulation using the Polystar model give a very similar creep strain evolution compared to the model without history effects (see Fig. 7). However, once the overheating stage has been performed, different creep strain predictions are observed since the Polystar model takes explicitly into account the progressive evolutions of the strengthening γ' phase whereas the model without history effects considers that the microstructure is immediately at thermodynamical equilibrium after the overheatings.

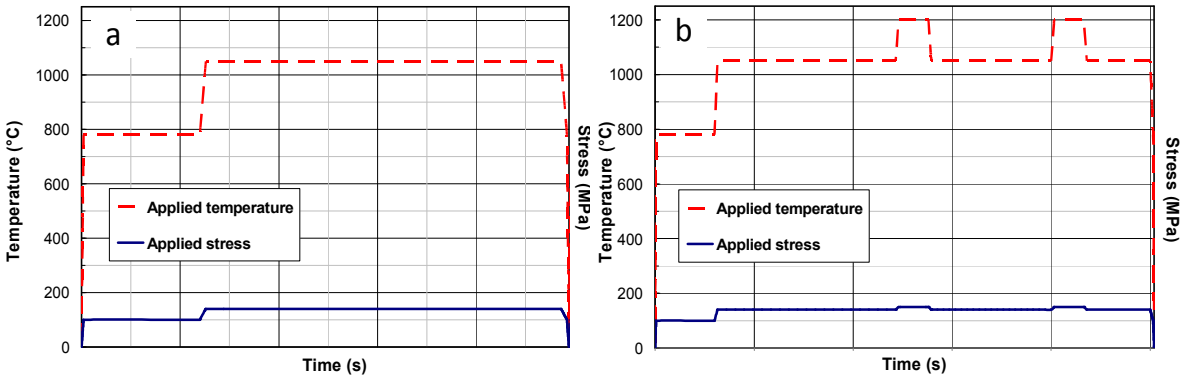

Figure 6: Mission test with the first block (a) cycled 100 times before the overheating block (b) and then cycled again 100 times.

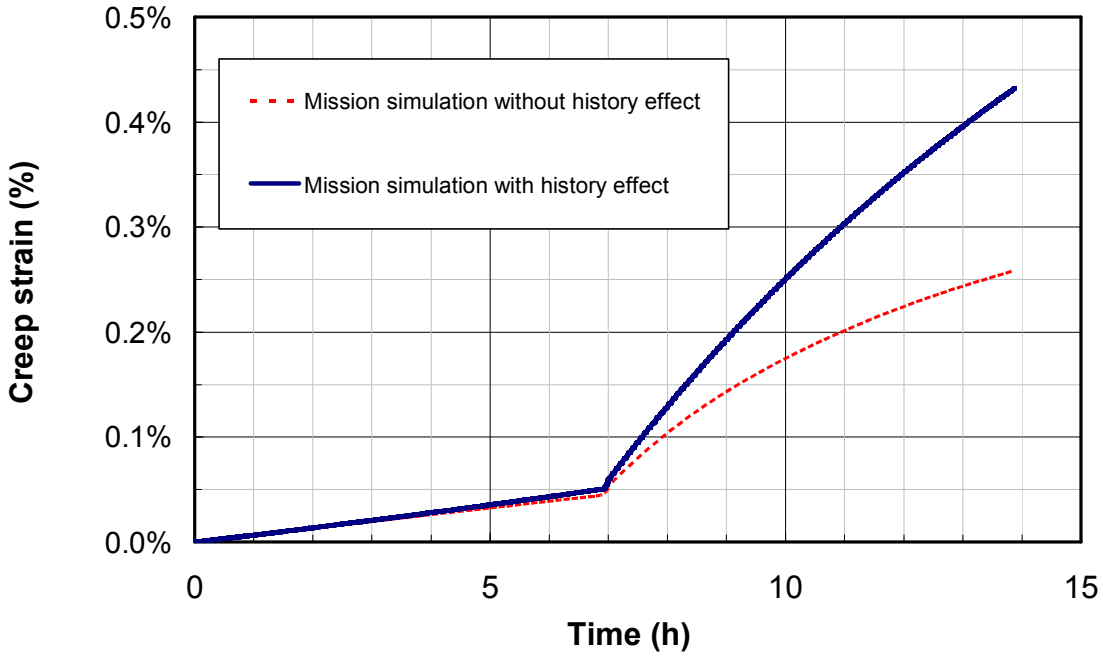

Figure 7: Creep strain predictions using the thermomechanical loading presented in Figure 6 and using either the Polystar model or a classical model which does not take into account microstructure evolutions.

Moreover, the Polystar model can be used for the computation of the γ' volume fraction of each kind of γ' particles (i.e. coarse non-fully-dissolved γ' precipitates f_l and small γ' re-precipitation f_s). Examples of such evolution have already been published previously (Cormier and Cailletaud (2010b)). It is expected to use in a near future such calculations as a reliable mean for the evaluation of component metal temperature under very high temperature loading paths.

4.2. First Limitation: Effect of the γ' Rafting

Complex thermomechanical tests have been achieved on different MC2 samples. These creep tests under constant load were conducted under thermal cycling conditions. The repeated cycle is presented in Figure 8.

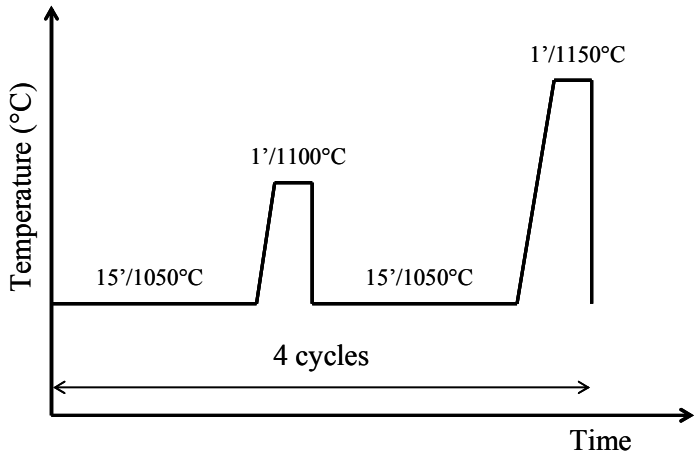

Figure 8: Test with pre-rafting and thermal cycling 4 times.

This thermal cycling was performed either on the as-received microstructure (i.e. a cuboidal microstructure) or on a rafted one (i.e. an isothermal creep test was performed prior to any thermal cycling). The reader is referred to Cormier et al. (2010c) for additional details. The creep strain evolutions as a function of time and of the microstructure at the beginning of thermal cycling are presented in Figure 9.

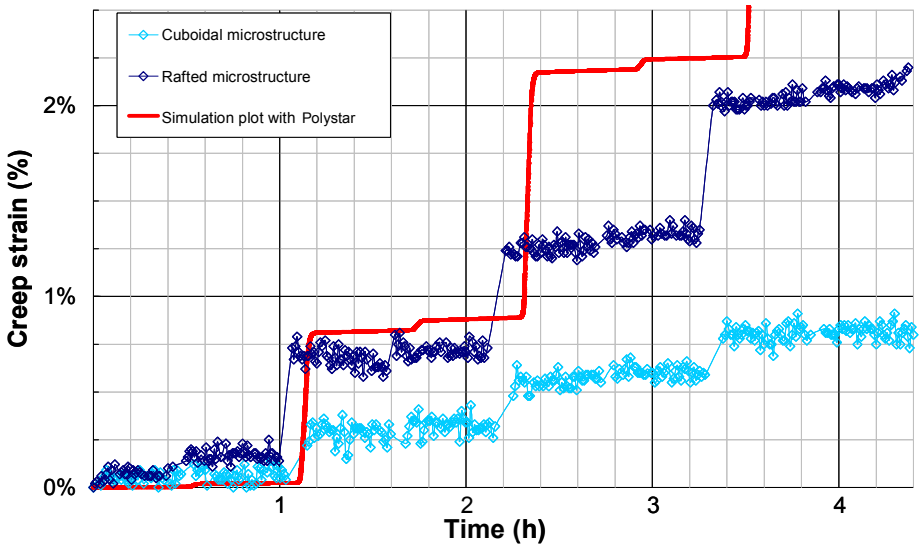

Figure 9: Experimental creep strains (dotted lines) – rafted microstructure (dark blue) and cuboidal microstructure (light blue) monitored during creep under thermal cycling conditions presented in Fig. 8 and corresponding model simulation (bold line) for the two conditions.

The present Polystar model, including its new modifications, is not able to capture the effect of the strengthening particle morphology since no internal variable describes this parameter. Indeed, the morphology of the microstructure does not induce the same creep resistance of the material and the same deformation mechanisms depending on the loading condition (see, e.g., Fedelich, et al. (2009)). This rafting effect explains the strain discrepancy between the two experimental plots. Moreover, as the effect of the fine precipitation is not activated in this simulation (Eqs. (13), (14) and (15)), the creep strain jumps at each temperature jump are higher than their experimental counterparts (i.e. experiment with a γ' rafted morphology). Indeed, it was recently observed that the hyperfine γ' precipitation nucleating after cooling from a higher temperature may lead to a strengthening effect which induces a decrease of creep strain (Le Graverend et al. (2010)).

The other effect of the γ' rafting has been identified on samples, the orientations of which are away from the classical [001] crystallographic orientation. An example of the typical creep behaviour of a near-[011] oriented MC2 sample (deviation from the [001]-[011] boundary less than 6 degrees) at 1050°C/140 MPa is presented in Figure 10. One can notice the incubation period in the first hours of creep where the microstructure remains almost cuboidal. Once the γ' rafting starts in two different <100> directions with one predominant due to the small secondary orientation in this case (see Fig. 10b), the material starts to creep faster with a rapid transition to the tertiary creep stage. The first hours are well predicted by the Polystar for this [011] crystal orientation (see Fig. 10a). However, the model misses the deformation increase once γ' rafting starts. One could have considered the activation of cubic slip system whose Schmid factor is non-negligible for this orientation. However, we remember here that this type of slip system is not relevant for the high/very temperature creep of [011] Ni-based single crystal superalloys (Sass and Feller-Kniepmeier (1998) and Han et al. (2010)). According to MacLachlan et al. (2000) and to Han et al. (2010), <112> {111} slip systems should also be considered. These systems are activated above a given threshold stress when the γ' phase starts to deform plastically. In addition to an additional modification of our model to take into account the effect of γ' rafting in the γ channel width evolution (modification of Eq. (11)), the activation of such systems could be a reliable way to capture the strain rate increase just after the incubation period observed in the first hours of creep deformation in Fig. 10a.

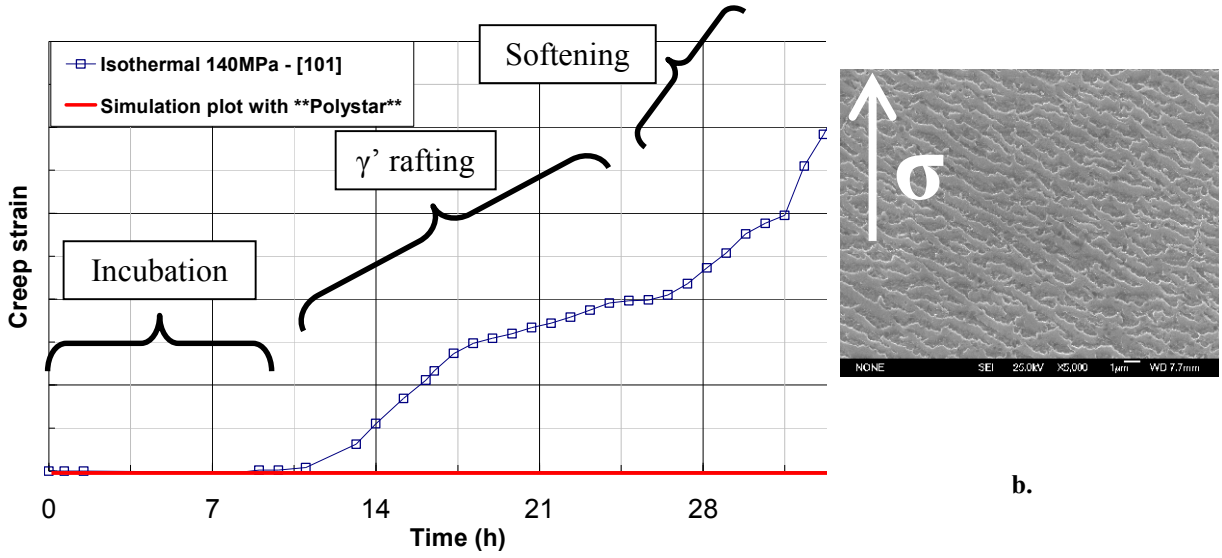

Figure 10: Isothermal creep tests for a near-[101] crystal orientation – (a): experimental plot (dotted line) compared to the simulation and (b): γ/γ' microstructure observed at failure out of the necking section along a (100) crystallographic plane.

Finally, once the γ' rafting is completed, a softening of the material is observed which leads to material failure. Final failure occurs along a (001) crystallographic plane due to microcracking nucleating from casting pores and subsequent crack propagation along the γ/γ' interfaces of the rafted microstructure (Ghighi (2012)).

4.3. Second Limitation: Effect of the Crystal Rotation

Finally, the last limitation encountered is correlated to the progressive crystallographic rotation occurring during creep for orientations far from stable ones such as [001] and [111]. Indeed, a crystal orientation mapping along the stress axis after creep failure of a [563] initially oriented MC2 sample shows such a progressive rotation of the local crystallographic orientation (Fig. 11). This characterisation was performed by means of EBSD mapping along a longitudinal section of failed samples. Along the gauge length of the failed sample, it is observed a progressive re-orientation from the initial [563] orientation close to the sample heads toward a [111] orientation close to the failure (see Figure 11). A 20 degrees rotation could have been measured in this particular case between the head of the sample and the fracture surface. This phenomenon was already noticed by Matan et al. (1999), MacLachlan et al. (2002) and Ardanaki et al. (1998) and needs to be taken into account. In fact, since the Polystar model is presently formulated under small strain assumptions, the orientation tensor is fixed and does not evolve according to the plastic strain rate tensor, as proposed by Asaro (1983, 1983a), Shenoy et al. (2008) or Staroselsky and Cassenti (2010). As a consequence, the evolution of the Young's modulus as a function of the plastic strain (i.e. the actual orientation) is not taken into account, which leads to severe underestimation of the plastic strain rate during the tertiary creep stage of orientation away from [001] and [111] ones. We feel that the last stages of creep deformation termed "softening" in Figure 10 could also be better predicted by taking into account such a rotation.
Introducing crystal rotation in the Polystar model is currently under progress.

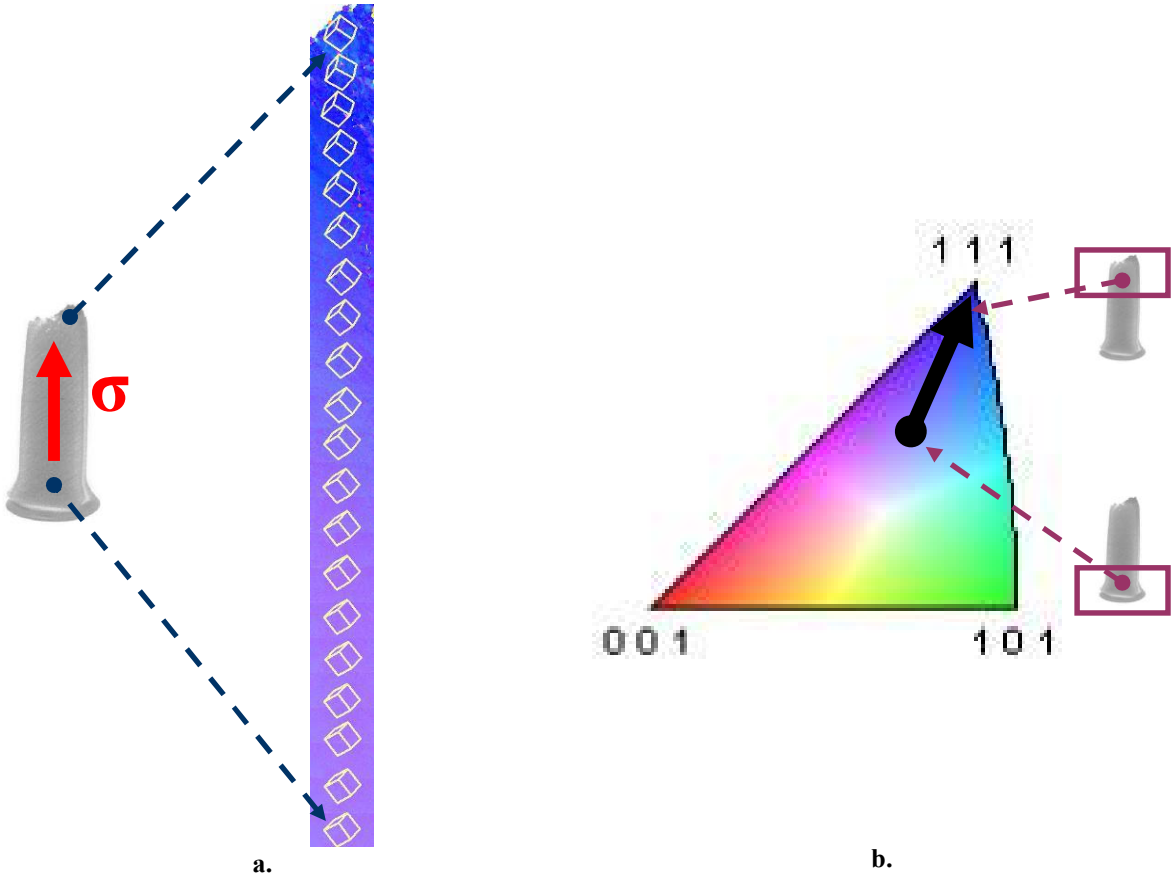

Figure 11: Orientation mapping along the stress axis performed by EBSD after an isothermal creep test on a [563] crystal orientation (a) and corresponding crystal rotation between the head of the sample and the fracture zone visualized on a standard stereographic triangle (b).

5. Conclusion

This paper discusses an extension of the Polystar crystal plasticity model to improve its capabilities for the prediction of non-isothermal creep behaviour and life of Ni-based single crystal superalloys. This is achieved by introducing new internal variables per slip system along with a modification of the constitutive equations. The

resulting model is capable of modelling with a good agreement all three stages of the creep of single crystal superalloys.

Three main improvements were added to the Polystar model and allow for

1. a strong coupling between γ' phase evolutions and plasticity. It allows a better description of the non-isothermal creep experiments, especially in the first stages of creep deformations where the microstructure progressively transforms from cuboidal particles to lamellar ones.
2. a better description of the progressive tertiary creep stages occurring under low temperatures.
3. reaching quite large (~10%) creep strains at failure that are now closer to experimental ones.

The results show a good agreement with the experimental data for the technologically most important [001] orientation, and demonstrate the applicability of the extended model for the simulation of primary, secondary and tertiary creep, and the estimation of lifetime of Ni-based single crystal superalloys under very complex thermomechanical loadings.

Still, two limitations remain and need to be taken into account: the effect of crystal rotation during tertiary creep of samples whose orientation is unstable, and the effect of the γ' morphology (e.g. cuboidal particles vs. rafted particles) on the mechanical properties.

Acknowledgements

This work is conducted under a French program involving Snecma-SAFRAN group, Turbomeca-SAFRAN group, ONERA, CNRS laboratories (Mines ParisTech, Institut P'-ENSMA, LMT-Cachan, LMS-X, CIRIMAT-ENSIACET) and CEAT. The authors are grateful to Turbomeca-SAFRAN group for sponsoring this work. J.G., E.O-K. and J.C. are grateful to Hervé Chalons (Methods Department at Turbomeca – SAFRAN group) for partial supervision of J.G. PhD Thesis and to Dr. Zeline Hervier (Materials Department at Turbomeca–SAFRAN group) for her continuous interest in this work. J.G. and J.C. are grateful to Pr. Patrick Villechaise (Institut P', UPR CNRS 3346, ENSMA, France) for his assistance in the EBSD characterisations.
The authors are very grateful to the editor and to Thomas Lederlin (Turbomeca – SAFRAN group) for their careful revisions of the manuscript.

References

Ardakani, M.; Ghosh, R.; Brien, V.; Shollock, B.; McLean, M.: Implications of dislocation micromechanisms for changes in orientation and shape of single crystal superalloys. *Scripta Mater.*39, (1998), 465–472.

Asaro, R.: Crystal plasticity. *J. App. Mech. - Trans. of the ASME*, 50, (1983), 921–934.

Asaro, R.: Micromechanics of crystals and polycrystals. *Adv. App. Mech.*, 23, (1983a), 1–115.

Cailletaud, G.: *Modélisation mécanique d'instabilités microstructurales en viscoplasticité cyclique à température variable*. Ph.D. thesis, ONERA (1979).

Cailletaud, G.: A micromechanical approach to inelastic behaviour of metals. *Int. J. Plast.*, 8, (1992), 55–73.

Carroll, L. J.; Feng, Q.; Pollock, T. M.: Interfacial dislocation networks and creep in directional coarsened Ru-containing nickel-base single-crystal superalloys. *Met. Mat. Trans. A*, 39A, (2008), 1290–1307.

Cormier, J.: *Comportement en fluage anisotherme à haute et très haute température du superalliage monocristallin MC2*. Ph.D. thesis, Ecole Nationale Supérieure de Mécanique et d'Aérotechnique & Université de Poitiers (2006).

Cormier, J.; Cailletaud, G.: Constitutive modeling of the creep behavior of single crystal superalloys under non-isothermal conditions inducing phase transformations. *Mat. Sci. Eng., A*527, (2010a), 6300–6312.

Cormier, J.; Cailletaud, G.: Constitutive modeling of the creep behaviour of single crystal superalloys under non-isothermal conditions inducing phase transformations. *Tech. Mech.*, 30, (2010b), 56–73.

Cormier, J.; Jouiad, M.; Hamon, F.; Villechaise, P.; Milhet, X.: Very high temperature creep behavior of a single crystal Ni-based superalloy under complex thermal cycling conditions. *Phil. Mag. Let.*, 90, (2010c), 611–620.

Cormier, J.; Milhet, X.; Vogel, F.; Mendez, J.: Non-isothermal creep behavior of a second generation Ni-based single crystal superalloy: experimental characterization and modeling. In: *SUPERALLOYS 2008,* pages 941-949 (2008).

Cormier, J.; Milhet, X.; Mendez, J.: Effect of very high temperature short exposures on the dissolution of the γ'-phase in single crystal MC2 superalloy. *J. Mat. Sci.*, 42, (2007a), 7780–7786.

Cormier, J.; Milhet, X.; Mendez, J.: Non-isothermal creep at very high temperature of the nickel-based single crystal superalloy MC2. *Acta Mat.*, 55, (2007b), 6250–6259.

Embury, J.; Deschamps, A.; Brechet, Y.: The interaction of plasticity and diffusion controlled precipitation reactions. *Scripta Mat.*, 49, (2003), 927 – 932.

Fedelich, B.: A microstructural model for the monotonic and the cyclic mechanical behavior of single crystals of superalloys at high temperatures. *Int. J. Plast.*, 18, (2002), 1–49.

Fedelich, B.; Künecke, G.; Epishin, A.; Link, T.; Portella, P.: Constitutive modelling of creep degradation due to rafting in single crystal Ni-base superalloys. *Mat. Sci. Eng., A*510-511, (2009), 273–277.

Fredholm, A.: *Monocristaux d'alliages base nickel : relation entre composition, microstructure et comportement en fluage à haute température*. Ph.D. thesis, Ecole Nationale Supérieure des Mines de Paris (1987).

Ghighi, J.: *Modélisation 3D de l'effet des évolutions microstructurales sur la durée de vie en fluage des alliages monocristallins*. Ph.D. thesis, Ecole Nationale Supérieure de Mécanique et d'Aérotechnique, Poitiers, France (2012)

Giraud, R.; Hervier, Z.; Cormier, J.; Martin, G. S.; Hamon, F.; Milhet, X.; Mendez, J.: Strain effect on the γ' dissolution at high temperatures of a nickel-based single crystal superalloy. *To be published* (2012).

Han, G.; Yu, J.; Sun, Y.; Sun, X.; Hu, Z.: Anisotropic stress rupture properties of the nickel-base single crystal superalloy SRR99. *Mat. Sci. Eng., A*527, (2010), 5383 – 5390.

Le Graverend, J.-B.; Cormier, J.; Jouiad, M.; Gallerneau, F.; Paulmier, P.; Hamon, F.: Effect of fine γ' precipitation on non-isothermal creep and creep-fatigue behaviour of nickel base superalloy MC2. *Mat. Sci. Eng., A*527, 20, (2010), 5295 – 5302.

Leidermark, D.; Moverare, J.; Simonsson, K.; Sjöström, S.; Johansson, S.: Room temperature yield behaviour of a single-crystal nickel-base superalloy with tension/compression asymmetry. *Comp. Mat. Sci.*, 47, (2009), 366 – 372.

Link, T.; Epishin, A.; Brückner, U.; Portella, P.: Increase of misfit during creep of superalloys and its correlation with deformation. *Acta Mat.*, 48, (2000), 1981 – 1994.

MacLachlan, D.; Wright, L.; Gunturi, S.; Knowles, D.: Modelling the anisotropic and biaxial creep behaviour of Ni-base single crystal superalloys CMSX-4 and SRR99 at 1223K. In: *SUPERALLOYS 2000*, pages 357–366 (2000).

MacLachlan, D. W.; Gunturi, G. S. K.; Knowles, D. M.: Modelling the uniaxial creep anisotropy of nickel base single crystal superalloys CMSX-4 and RR2000 at 1023K using a slip system based finite element approach. *Comp. Mat. Sci.*, 25, (2002), 129–141.

MacLachlan, D. W.; Wright, L. W.; Gunturi, G. S. K.; Knowles, D. M.: Constitutive modelling of anisotropic creep deformation in single crystal blade alloys SRR99 and CMSX-4. *Int. J. Plast.*, 17, (2001), 441–467.

Matan, N.; Cox, D. C.; Carter, P.; Rist, M. A.; Rae, C. M. F.; Reed, R. C.: Creep of CMSX-4 superalloy single crystals: effects of misorientation and temperature. *Acta Mat.*, 47, (1999), 1549–1563.

McLean, M.; Dyson, B.: Modeling the effects of damage and microstructural evolution on the creep behavior of engineering alloys. *J. Eng. Mat. Tech.*, 122, (2000), 273–278.

Norton, F.: *In creep of steel at high temperatures* (1929).

Peirce, D.; Asaro, R.; Needleman, A.: An analysis of non-uniform and localized deformation in ductile single-crystals. *J. Met.*, 34, (1982), 32–33.

Probst-Hein, M.; Dlouhy, A.; Eggeler, G.: Dislocation interactions in gamma-channels between γ'-particles of superalloy single crystals. *Mat. Sci. Eng., A*319-321, (2001), 379 – 382.

Reed, R.: *The Superalloys - Fundamentals and Applications* . Cambridge University Press (2006).

Reed, R.; Cox, D.; Rae, C.: Damage accumulation during creep deformation of a single crystal superalloy at 1150°C. *Mat. Sci. Eng., A*448, (2007), 88 – 96.

Sarosi, P.; Srinivasan, R.; Eggeler, G.; Nathal, M.; Mills, M.: Observations of a<010> dislocations during the high-temperature creep of Ni-based superalloy single crystals deformed along the [001] orientation. *Acta Mat.*, 55, (2007), 2509 – 2518.

Sass, V.; Glatzel, U.; Feller-Kniepmeier, M.: Creep anisotropy in the monocrystalline nickel-base superalloy CMSX-4. In: *Superalloys 1996*, pages 283–290 (1996).

Sass, V.; Feller-Kniepmeier, M.: Orientation dependence of dislocation structures and deformation mechanisms in creep deformed CMSX-4 single crystals. *Mat. Sci. Eng., A*245, (1998), 19–28.

Shenoy, M.; Tjiptowidjojo, Y.; McDowell, D.: Microstructure-sensitive modeling of polycrystalline in 100. *Int. J. Plast.*, 24, (2008), 1694–1730.

Srinivasan, R.; Eggeler, G.; Mills, M.: γ'-cutting as rate-controlling recovery process during high-temperature and low-stress creep of superalloy single crystals. *Acta Mat.*, 48, (2000), 4867 – 4878.

Staroselsky, A.; Cassenti, B.: Combined rate-independent plasticity and creep model for single crystal. *Mech. of Mat.*, 42, (2010), 945–959.

Staroselsky, A.; Cassenti, B. N.: Mechanisms for tertiary creep of single crystal superalloy. *Mech. Time Dep. Mat.*, 12, (2008), 275–289.

Staroselsky, A.; Cassenti, B. N.: Creep, plasticity, and fatigue of single crystal superalloy. *Int. J. Sol. Struct.*, 48, (2011), 2060 – 2075.

Svoboda, J.; Lukás, P.: Model of creep in <001>-oriented superalloy single crystals. *Acta Mat.*, 46, (1998), 3421 – 3431.

Vladimirov, I. N.; Reese, S.; Eggeler, G.: Constitutive modelling of the anisotropic creep behaviour of nickel-base single crystal superalloys. *Int. J. Mech. Sci.*, 51, 4, (2009), 305 – 313.

Wen, Z.; Hou, N.; Yue, Z.: Creep damage and crack initiation behaviour of nickel-base single crystalline superalloys compact tension specimen with a void ahead of crack tip. *Mat. Sci. Eng., A*510-511, (2009), 284–288.

Yu, Q.; Yue, Z.; Wen, Z.: Creep damage evolution in a modeling specimen of nickel-based single crystal superalloys air-cooled blades. *Mat. Sci. Eng., A*477, (2008), 319–327.

Addresses: Julien Ghighi (Ing.-M.Sc) and Dr.-Ing. Elisabeth Ostoja-Kuczynski, Turbomeca –SAFRAN group, Methods Department, Avenue Joseph Szydlowski, 64511 Bordes Cedex, France.
email: julien.ghighi@turbomeca.fr; elisabeth.ostoja-kuczynski@turbomeca.fr

Dr.-Ing. Jonathan Cormier and Dr.-Ing. José Mendez, Institut Pprime, UPR CNRS 3346, Département Physique et Mécanique des Matériaux, ENSMA, BP 40109, 86961 Futuroscope Chasseneuil Cedex, France
email: jonathan.cormier@ensma.fr; jose.mendez@ensma.fr

Prof. Georges Cailletaud and Dr. Farida Azzouz, MINES Paris Tech, Centre des Matériaux, UMR CNRS 7633, BP 87, 91003 Evry Cedex, France
email: georges.cailletaud@ensmp.fr; farida.azzouz@ensmp.fr